

## Characterization of Zn-doped hematite thin films for photoelectrochemical splitting of water

Saroj Kumari<sup>1</sup>, Chanakya Tripathi<sup>2</sup>,  
Aadesh P. Singh<sup>1</sup>, Diwakar Chauhan<sup>2</sup>,  
Rohit Shrivastav<sup>2</sup>, Sahab Dass<sup>2</sup> and  
Vibha R. Satsangi<sup>1,\*</sup>

<sup>1</sup>Department of Physics and Computer Science and

<sup>2</sup>Department of Chemistry, Faculty of Science, Dayalbagh Educational Institute, Dayalbagh, Agra 282 005, India

**Hydrogen production using the photoelectrochemical (PEC) route promises to be a clean and efficient way of storing solar energy for use in hydrogen-powered fuel cells. Iron oxide ( $\alpha$ -Fe<sub>2</sub>O<sub>3</sub>) is best suited to be used as a photoelectrode in PEC cells for solar hydrogen production due to its favourable bandgap of ~2.2 eV, lying in visible region. The present communication describes the PEC study on Zn-doped  $\alpha$ -Fe<sub>2</sub>O<sub>3</sub> thin films prepared by spray pyrolytic method at different doping concentrations (0.5, 1.0, 1.5, 5.0 and 10.0 at%). Photocurrent density was found to depend upon the doping concentration of Zn. Maximum photocurrent density of ~0.64 mA cm<sup>-2</sup> at an applied potential of 0.7 V/SCE was observed for 5.0 at% doping concentration. All the samples of doped/undoped  $\alpha$ -Fe<sub>2</sub>O<sub>3</sub> were characterized for phase formation, particle size, nature of charge carrier, bandgap, resistivity and carrier density. The flatband potential of -0.78V/SCE and depletion layer width of 28.7 Å were calculated from the Mott-Schottky plot for 5.0 at% doping concentration.**

**Keywords:** Flatband potential, hematite, hydrogen, photoelectrochemical route.

THE semiconductor/electrolyte interface has been a field of intense research in the past few years, especially in view of the important challenge of photoelectrochemical (PEC) conversion of solar energy into hydrogen fuel by splitting of water using semiconductor electrodes in which photoinduced electrochemical reactions are carried out. Photoexcitation of the semiconductor with solar energy greater than the bandgap of the semiconductor generates electron-hole pairs at the semiconductor–electrolyte interface. Light-induced electron–hole pairs drive a chemical reduction and an oxidation reaction in the electrolyte of the PEC system, leading to hydrogen and oxygen evolution (water-splitting). In this situation the photon energy is converted directly into chemical energy rather than into intermediate electrical energy as with solid-state or electrochemical PV cells.

Hematite ( $\alpha$ -Fe<sub>2</sub>O<sub>3</sub>) is an attractive material for PEC studies due to its bandgap ( $E_g = 2.2$  eV), lying nearly in

the optimum range for solar splitting of water. This bandgap allows absorption of solar energy in the visible region, where the sun emits maximum energy. Besides,  $\alpha$ -Fe<sub>2</sub>O<sub>3</sub> is naturally abundant in the earth's crust and is therefore, a low cost material. It is also corrosion-resistant in acidic and alkaline medium<sup>1</sup>.

On account of these favourable characteristics, many authors have studied the potential of using hematite in solar-energy conversion prepared by different routes, e.g. pressing of material into pellets<sup>2–4</sup>, sputtering<sup>5</sup> and spray pyrolysis<sup>6,7</sup>. Nanostructured and nanorods of hematite have also been studied for photoelectrochemical splitting of water<sup>8,9</sup>. However, the best photoresponse has been reported for hematite prepared by spray pyrolysis<sup>6,10</sup>. Low quantum efficiencies of hydrogen production in iron oxide-based PEC system is mainly due to an insufficient negative flatband potential produced and/or low values of the charge carrier mobility due to hopping mechanism of conductivity.

Pilot experiments were carried out on  $\alpha$ -Fe<sub>2</sub>O<sub>3</sub> doped with many dopants, and the best photocurrent was observed for  $\alpha$ -Fe<sub>2</sub>O<sub>3</sub> doped with Zn. In the present communication, Zn-doped  $\alpha$ -Fe<sub>2</sub>O<sub>3</sub> photoelectrodes have been prepared by spray pyrolysis method, investigated in detail for their photoresponse in PEC cells and characterized for various parameters affecting the PEC splitting of water.

Thin films were deposited on conducting glass (SnO<sub>2</sub>:F-coated) substrates by spraying 0.15 M precursor solution, prepared by dissolving Fe(NO<sub>3</sub>)<sub>3</sub>·9H<sub>2</sub>O (99.9%, Aldrich) with varying dopant concentrations (0.5, 1.0, 1.5, 5.0 and 10.0 at%) of Zn(NO<sub>3</sub>)<sub>2</sub>·6H<sub>2</sub>O in double-distilled water. The solution was sprayed with air at a pressure of 10 kg/cm<sup>2</sup> onto heated (temperature 350 ± 5°C) glass substrate, with nearly one-third length of the substrate initially covered by an aluminum foil. Finally, all samples were sintered at 500°C for 2 h. Sintering helps the samples in attaining crystallinity, increases particle/grain size and decreases resistivity of the film. Using silver paint and copper wire loop, ohmic electrical contacts were generated on the uncoated conducting substrate surface for PEC measurements.

PEC measurements involved current–voltage ( $I$ – $V$ ) characteristics under darkness and illumination of PEC cell consisting of samples of iron oxide doped with zinc as working electrode using a potentiostat (Model Versa Stat II, U.S.A) and Xe lamp (150 Watt, Bentham). NaOH (13 pH) was used as electrolyte. Photocurrent densities as calculated from  $I$ – $V$  data, are observed to increase with increasing doping concentration (Figure 1). The 5 at% Zn doping offered the best photocurrent density. It seems that the 5 at% Zn doping in Fe<sub>2</sub>O<sub>3</sub> is the optimal concentration above which (for 10 at% Zn) the observed photocurrent density decreases.

$I$ – $V$  characteristic and Mott–Schottky plots (Figure 2) of all samples of iron oxide clearly indicate the  $n$ -type conductivity of the material. Khan and co-workers<sup>11</sup> on the other hand, have reported Zn-doped Fe<sub>2</sub>O<sub>3</sub> prepared by spray pyrolysis method using iron(III) chloride as  $p$ -

\*For correspondence. (e-mail: vibhasatsangi@rediffmail.com)

type. They also showed that Zn helped in converting the indirect bandgap of  $\text{Fe}_2\text{O}_3$  to direct bandgap due to formation of  $\text{ZnFe}_2\text{O}_4$ . This difference may be due to the condition of preparation and selection of precursor chemical.

Flatband potential of semiconductor electrode at the semiconductor–electrolyte interface is an important parameter in designing a PEC cell; larger the flatband potential, easier is the transfer of carriers at the interface. This can be obtained from the Mott–Schottky plot ( $1/C_{sc}^2$  vs electrode potential), which relates the capacitance of space charge layer ( $C_{sc}$ ) to the applied potential ( $V_{app}$ ), assuming that capacitance of the double layer at the semiconductor–electrolyte interface is much smaller<sup>12–14</sup>, using the following equation:

$$1/C_{sc}^2 = [2/q\epsilon_s\epsilon_0 N_D] [V_{app} - V_{FB} - (k_B T/q)], \quad (1)$$

where  $q$  is charge on the carriers,  $\epsilon_s$  the permittivity of semiconductor electrode,  $\epsilon_0$  the permittivity of free space,  $N_D$  the donor density,  $V_{FB}$  the flatband potential,  $k_B$  the Boltzmann's constant and  $T$  the temperature of operation.

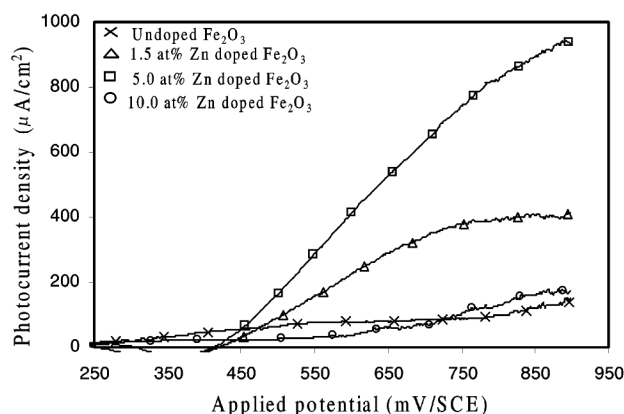


**Figure 1.** Photo-current density–voltage (mV/SCE) characteristics for Zn-doped  $\text{Fe}_2\text{O}_3$  using 150 W Xe lamp as light source. Dependence of photocurrent density on different doping concentrations (at%) in 13 pH NaOH electrolyte solution.

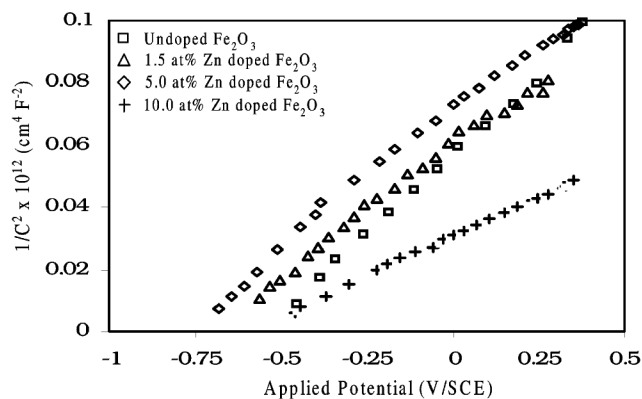


**Figure 2.** Dependence of Mott–Schottky plot on different doping concentrations (at%) at frequency 1 kHz; electrolyte solution 13 pH NaOH.

LCR meter Model-4263B Agilent Technology, Singapore, was utilized for measurement of capacitance ( $C_{sc}$ ) at the semiconductor–electrolyte junction in PEC cell at 1 kHz frequency and Mott–Schottky curves were obtained (Figure 2). Flatband potentials and donor densities were calculated from the intercept and slope of the Mott–Schottky plots respectively. Both were found to vary by changing the doping concentration (Table 1). It has been observed that the level of doping up to 5 at% increases the flatband potential, suggesting the better ability of the film to facilitate the charge carrier from semiconductor to electrolyte.

Resistivity as calculated from the  $I$ – $V$  characteristics was found to increase after doping. Increase in resistivity may be attributed due to the incorporation of doping metal ions ( $\text{Zn}^{++}$ ) into  $\text{Fe}_2\text{O}_3$  causing the loss of an electron (Table 1).

Depletion layer width of semiconductor–electrolyte interface was determined from capacitance measurement across the junction at zero applied voltage using the formula:

$$w = \epsilon_s \epsilon_0 / C_{sc}, \quad (2)$$

where  $\epsilon_s$  is the permittivity of semiconductor electrode,  $\epsilon_0$  the permittivity of free space and  $C_{sc}$  the space charge capacitance. It was observed that doping up to 5 at% increases the depletion layer width, after which it again decreases (Table 1).

**Table 1.** Resistivity and flatband potential ( $V_{FB}$ ), donor density ( $N_D$ ) and depletion layer width ( $w$ )

Sample detail	Resistivity ( $\Omega$ cm)	$V_{FB}$ (V/SCE)	$N_D$ ( $\text{cm}^{-3}$ )	$w$ ( $\text{\AA}$ )
Undoped	$1.7 \times 10^6$	–0.58	$21.4 \times 10^{19}$	11.0
0.5 at%	$4.1 \times 10^7$	–0.66	$14.4 \times 10^{19}$	19.8
1.0 at%	$5.4 \times 10^7$	–0.69	$14.0 \times 10^{19}$	24.9
1.5 at%	$6.8 \times 10^7$	–0.71	$12.0 \times 10^{19}$	26.2
5.0 at%	$5.7 \times 10^7$	–0.78	$11.0 \times 10^{19}$	28.7
10.0 at%	$2.6 \times 10^7$	–0.59	$22.0 \times 10^{19}$	18.7

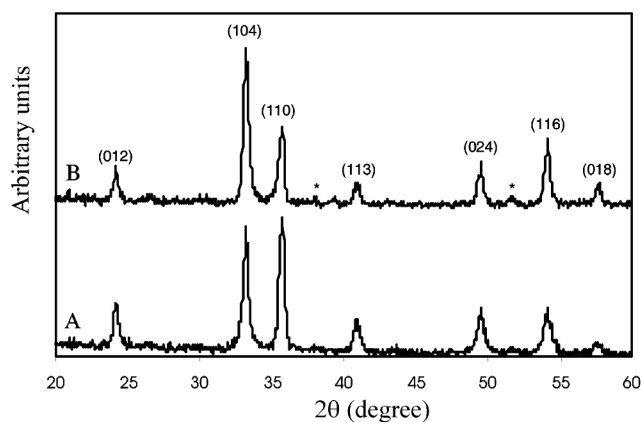


**Figure 3.** X-ray diffraction pattern of undoped  $\text{Fe}_2\text{O}_3$  (A) and 5.0 at% Zn-doped  $\text{Fe}_2\text{O}_3$  (B). Peaks corresponding to underlying  $\text{SnO}_2$ :F layer on the substrate.

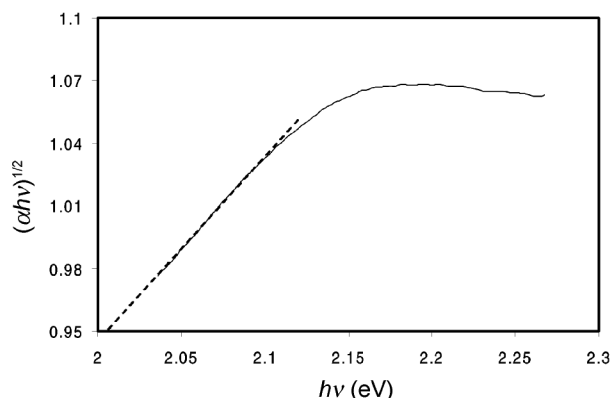


Figure 4.  $(\alpha hv)^{1/2}$  vs  $(hv)$  for 5 at% Zn-doped  $\text{Fe}_2\text{O}_3$  thin film.

Structural characterization of films was carried out using X-ray powder diffractometer (XRD; X'PERT Model, Philips, with graphite monochromator) using Cu-K $\alpha$  wavelength. Figure 3 illustrates the XRD patterns of undoped and 5 at% Zn-doped films of  $\text{Fe}_2\text{O}_3$ . All the samples of doped/undoped  $\alpha\text{-Fe}_2\text{O}_3$  prepared by spray pyrolysis method were found to be  $\alpha\text{-Fe}_2\text{O}_3$  (hematite). The average particle size calculated from XRD data using Scherrer's equation is of the order of 60 nm. Variation in doping concentration did not much affect the particle size.

Absorbance of thin films was recorded using UV-spectrophotometer (Shimadzu, UV-1601) and bandgap energies were calculated using the following equation<sup>15-17</sup>:

$$(\alpha hv) = A (hv - E_g)^n, \quad (3)$$

where  $\alpha$  is the absorption coefficient,  $A$  is a constant related to the effective mass of the electrons and holes, and  $n = 0.5$  for allowed direct transitions, and 2 for allowed indirect transitions,  $E_g$  is the energy gap. In the absorbance versus wavelength curve, the absorption edge was found at around 623 nm and the absorption peak was at around 560 nm. Within this wavelength range, the  $(\alpha hv)^{1/2}$  vs  $(hv)$  plot is linear (shown by solid line in Figure 4), indicating the indirect nature of the bandgap. This linear trend was extrapolated (dotted line) to the  $hv$  axis to calculate the bandgap.

The band gap was found to be approximately the same for all samples,  $\sim 2.0$  eV. Zn may not produce any intermediate level within the energy level of iron oxide.

In the present study, Zn doping of  $\text{Fe}_2\text{O}_3$  has yielded samples with better photoresponse, increased resistivity, decreased donor density and increased flatband potential at the semiconductor-electrolyte junction. Increase in flatband potential helps in transfer of charge carriers at the interface, and increase in depletion layer width at the junction increases the absorption of incident light energy. These two factors may be responsible for a better photoresponse. Highest photocurrent density is obtained in case of 5 at% Zn-doped  $\text{Fe}_2\text{O}_3$ , which appears an optimal doping concentration. The photoresponse for 10 at% Zn-doped

$\text{Fe}_2\text{O}_3$  thin film again decreases due to decrease in flatband potential and depletion layer width.

1. Yeh, L. S. R. and Hackerman, N., Iron-oxide semiconductor electrodes in photoassisted electrolysis of water. *J. Electrochem. Soc., Electrochem. Sci. Technol.*, 1977, **124**, 833-836.
2. Leygraf, C., Hendewerk, M. and Somorjai, G. A., Mg- and Si-doped iron oxides for the photocatalyzed production of hydrogen from water by visible light ( $2.2 \text{ eV} < hv < 2.7 \text{ eV}$ ). *J. Catal.*, 1982, **78**, 341-351.
3. Gurunathan, K. and Maruthamuthu, P., Photogeneration of hydrogen using visible light with undoped/doped  $\alpha\text{-Fe}_2\text{O}_3$  in the presence of methyl viologen. *Int. J. Hydrogen Energy*, 1995, **20**, 287-295.
4. Aroutiounian, V. M., Arakelyan, V. M., Shahnazaryan, G. E., Stepanyan, G. M., Turner, J.A. and Khaselev, O., Investigation of ceramic ( $\text{Fe}_2\text{O}_3/\text{Ta}$ ) photoelectrodes for solar energy photoelectrochemical converters. *Int. J. Hydrogen Energy*, 2002, **27**, 33-38.
5. Virtanen, S., Schmuki, P., Böhni, H., Vuoristo, P. and T., Artificial Cr- and Fe-oxide passive layers prepared by sputter deposition. *J. Electrochem. Soc.*, 1995, **142**, 3067-3072.
6. Khan, S. U. M. and Akikusa, J., Photoelectrochemical splitting of water at nanocrystalline  $n\text{-Fe}_2\text{O}_3$  thin-film electrodes. *J. Phys. Chem. B*, 1999, **103**, 7184-7189.
7. Lindgren, T., Vayssieres, L., Wang, H. and Lindquist, S.-E., *Chemical Physics of Nanostructured Semiconductors* (eds Kokorin, A. I. and Bahnmann, D. W.), VSP, Utrecht, The Netherlands, 2003, pp. 93-126.
8. Björkstén, U., Moser, J. and Grätzel, M., Photoelectrochemical studies on nanocrystalline hematite films. *Chem. Mater.*, 1994, **6**, 858-863.
9. Vayssieres, L., Beermann, N., Lindquist, S.-E. and Hagfeldt, A., Controlled aqueous chemical growth of oriented three-dimensional nanorod arrays: application to iron(III) oxides. *Chem. Mater.*, 2001, **13**, 233-235.
10. Ingler Jr. W. B. and Khan, S. U. M., Photoresponse of spray pyrolytically synthesized magnesium-doped iron(III) oxide ( $p\text{-Fe}_2\text{O}_3$ ) thin films under solar simulated light illumination. *Thin Solid Films*, 2004, **461**, 301-308.
11. Ingler Jr. W. B., Baltrus, J. P. and Khan, S. U. M., Photoresponse of  $p$ -type zinc-doped iron(III) oxide thin films. *J. Am. Chem. Soc.*, 2004, **126**, 10238-10239.
12. Wilhelm, S. M., Yun, K. S., Ballenger, L. W. and Hackerman, N., Semiconductor properties of iron-oxide electrodes. *J. Electrochem. Soc., Electrochem. Sci. Technol.*, 1979, **126**, 419-424.
13. Kocha, S. S., Turner, J. A. and Nozik, A. J., Study of the Schottky barrier and determination of the energetic positions of band edges at the  $n$ - and  $p$ -type gallium indium phosphide electrode electrolyte interface. *J. Electroanal. Chem.*, 1994, **367**, 27-30.
14. Kennedy, J. H. and Frese, K. W., Flatband potentials and donor densities of polycrystalline  $\alpha\text{-Fe}_2\text{O}_3$  determined from Mott Schottky plots. *J. Electrochem. Soc., Electrochem. Sci. Technol.*, 1978, **125**, 723-726.
15. Misho, R. H. and Murad, W. A., Band gap measurements in thin films of hematite  $\text{Fe}_2\text{O}_3$ , pyrite  $\text{FeS}_2$  and troilite  $\text{FeS}$  prepared by chemical spray pyrolysis. *Solar Energy Mater. Solar Cells*, 1992, **27**, 335-345.
16. Chaudhary, Y. S., Agrawal, A., Shrivastav, R., Satsangi, V. R. and Dass, S., A study on the photoelectrochemical properties of copper oxide thin films. *Int. J. Hydrogen Energy*, 2004, **29**, 131-134.
17. Watabe, I. and Okumura, T., Annealing behavior of amorphous C:H films prepared by glow discharge decomposition of  $\text{CH}_4$  and  $\text{H}_2$ . *Jpn. J. Appl. Phys.*, 1986, **25**, 1851-1854.

ACKNOWLEDGEMENTS. We thank the Department of Science and Technology, New Delhi, for financial assistance. We also thank Dr R. K. Sharma, Solid State Physics Laboratory (DRDO), Delhi for XRD analysis of thin films.

Received 15 February 2006; revised accepted 26 June 2006